

In Vivo Cellular Imaging of Magnetically Labeled Hybridomas in the Spleen With a 1.5-T Clinical MRI System

Pierre Smirnov,^{1,2} Florence Gazeau,² Maité Lewin,¹ Jean Claude Bacri,² Nathalie Siauve,¹ Catherine Vayssettes,¹ Charles André Cuénod,¹ and Olivier Clément^{1*}

The feasibility of in vivo cellular imaging using a 1.5 T clinical magnet was studied in the mouse. Hybridoma cells were labeled with anionic γ -Fe₂O₃ superparamagnetic iron oxide nanoparticles. These were internalized by the endocytose pathway. Both electron spin resonance and magnetophoresis as a measure of the labeled cells migration velocity under a magnetic field were used to quantify particle uptake. A fast (<2 hr) and substantial (up to 5 pg of iron per cell) internalization of nanoparticles by hybridomas was found, with good agreement between the two methods used. Hybridomas labeled with 2.5 pg iron per cell were injected intraperitoneally to male Swiss nude mice. A decrease in the spleen signal, suggesting a “homing” of labeled hybridomas to this organ, was found 24 hr later by MRI performed at 1.5 T. Furthermore, in labeled cells recovered from the spleen by ex vivo magnetic sorting, a mean of 0.5 pg iron per cell was found, i.e., a value five times lower than that of the injected hybridomas. This finding is consistent with in vivo proliferation of these cells. In addition, the amount of labeled hybridomas present in the spleen was found to correlate with MRI signal intensity. Magn Reson Med 52:73–79, 2004. © 2004 Wiley-Liss, Inc.

Key words: 1.5 T MRI cell tracking; superparamagnetic anionic iron oxide nanoparticles; magnetophoresis and electron spin resonance

Cell labeling is finding increasing applications in fields such as cellular biology and medical imaging. Analysis of the distribution and cellular migration, or “cellular trafficking,” is essential for many physiological and pathological processes (1,2). Cell migration is a key phenomenon in the immune system, with continuous redistribution of lymphocytes towards various anatomical sites (3,4). Recirculation of lymphocytes facilitates their interactions with foreign antigens and inflammatory cells. Studies of T-lymphocyte redistribution in vivo are limited by the small number of anatomical sites that can be analyzed simultaneously and by the poor sensitivity of current markers.

Conventional methods based on marker proteins labeled with fluorescence probes or with radioisotopes (¹¹¹In, ¹²³I,

or ⁵¹Cr) can be used to study lymphocyte trafficking, but these methods are limited by the isotope half-life, the tracer transfer rate into cells, and the toxicity of the labeling process (1,5). A noninvasive method capable of following lymphocyte migration for prolonged periods in vivo, and particularly during the first 72 hr of the immune response, could be highly informative.

MRI can be used to follow labeled cells using an endogenous or exogenous contrast agent. The agent must be specific for a given cell type, must not affect the antigenic properties of the cell, must induce a specific local signal distinguishable from neighboring tissues, and persist on or inside the labeled cell for an adequate time. The best contrast agent for studying cellular migration is superparamagnetic particles (6,7), also known as superparamagnetic iron oxide (SPIO) or ultrasmall superparamagnetic iron oxide (USPIO). These particles have a remarkable r_2 relaxivity which makes them particularly effective on T_2 -weighted imaging. The most widely used product is dextran-coated superparamagnetic particles (8–10). T-lymphocytes can be labeled with superparamagnetic particles and visualized in vivo at the single-cell level (8). Cellular uptake by spontaneous endocytosis is not very efficient, but can be enhanced by the use of a peptide sequence of HIV-1 transactivator protein (Tat). This protein is internalized by cells when present in the extracellular medium (11,12). Tat peptide can be conjugated with superparamagnetic particles, resulting in nanoparticles with great stability and cellular permeability (13). The conjugate can also be labeled with a fluorochrome (FITC), enabling it to be visualized by both flow cytometry and high-resolution MRI (14). Other methods used to coat magnetic nanoparticles include monoclonal antibodies (15), transfection agents including dendrimers (16), and lipofection agents (17).

A new class of superparamagnetic anionic nanoparticles was recently described (18–20). They are not dextran-coated and carry negative surface charges, offering good stability in suspension due to electrostatic repulsion forces. Moreover, they show a high degree of uptake by different cell lines, secondary to their electrostatic accumulation on the cell membrane (21).

Here we developed a lymphocyte imaging method with a 1.5 T clinical MRI unit. We used a hybridoma cell line as a model and magnetically labeled the cells with the above-mentioned anionic nanoparticles. Nanoparticle uptake by hybridoma cells was quantified in vitro and their trafficking was visualized by MRI in the mouse spleen after i.p. injection.

¹Laboratoire de Recherche en Imagerie (LRI), Inserm U 494, Faculté de Médecine Necker, Paris, France.

²Laboratoire des Milieux Désordonnés et Hétérogènes (LMDH), CNRS UMR 7603, Universités Paris 6 et 7, Paris, France.

*Correspondence to: Olivier Clément, Laboratoire de Recherche en Imagerie, Inserm U 494, Faculté de Médecine Necker Enfants-Malades, 156 rue de Vaugirard, 5^{ème} étage, porte 1^{er}, 75015 Paris, France. E-mail: clement@necker.fr

Received 28 August 2003; revised 5 February 2004; accepted 5 February 2004.

DOI 10.1002/mrm.20121

Published online in Wiley InterScience (www.interscience.wiley.com).

© 2004 Wiley-Liss, Inc.

MATERIALS AND METHODS

Hybridomas

6B2 hybridomas were prepared by fusion between B lymphocytes and myeloma cells. They were cultured in RPMI 1640 medium (Gibco, Invitrogen Corporation) containing 10% fetal calf serum (FCS) (Gibco, Invitrogen, La Jolla, CA), 100 IU/mL penicillin, and 100 μ g/mL streptomycin (Gibco, Invitrogen). Flat-bottomed flasks with a surface area of 80 cm² (Cellstar, Greiner bio-one) were sown with 500,000 cells and placed at 37°C in a saturated atmosphere containing 5% CO₂. The cells grew in suspension and reached confluence within 3 days. The cell suspension was then homogenized by aspiration-repression with a sterile pipette. Viable cells were counted under a light microscope with a Malassez cell and Trypan blue (Gibco, Invitrogen).

Cell Labeling With Magnetic Nanoparticles

We used a colloidal suspension of iron oxide nanoparticles (maghemite γ -Fe₂O₃) dispersed in water (ferrofluid). These particles were synthesized according to Massart's method, by alkalization of ferrous and ferric chloride (22). They were then chelated by adding sodium citrate (10% per mole of iron) to the precursory acid ferrofluid, adsorption of which to the nanoparticle surface confers a negative total charge over a large range of pH values: the trisodium citrate has three carboxylate functions (pKa 2.8, 4.4, and 5.65) deprotonated at physiological pH. We obtained an aqueous solution of nanoparticles with negative charges carried by the carboxylate groups of the adsorbed citrate molecules. This conferred high stability to the colloidal suspension through electrostatic repulsion. The nanoparticles consisted of monocrystals of so-called maghemite (γ -Fe₂O₃) with a core of mean diameter 8 nm, carrying an effective magnetic moment $m_{eff} = M_s V$, where M_s is the magnetization of maghemite at saturation and V the volume of a particle ($M_s = 3.1 \times 10^5$ A/m²) (20).

Cultured hybridomas were suspended in RPMI medium containing 5 mM sodium citrate and distributed in Petri dishes (Cellstar, Greiner bio-one). The cells were then incubated at 37°C with the particles by adding the citrated solution of ferrofluid for various times (20 min to 6 hr) and with various iron concentrations in the incubation medium (0.25–15 mM). The presence of citrate in RPMI prevents particle aggregation by maintaining the surface density of negative charges. After incubation the supernatant was isolated, and two successive very mild washing steps were performed by addition-aspiration of citrated RPMI. The cells were then incubated with citrated RPMI for 1 hr at 37°C to allow them to internalize the particles (chase period). The cells were collected by scraping and resuspended before use in *in vitro* studies or injection into animals.

Quantification of Iron Uptake

Two methods were used to quantify the uptake of citrated nanoparticles by hybridoma cells, namely, magnetophoresis and electron spin resonance (ESR).

Magnetophoresis

Cells loaded with particles became magnetic and moved in the presence of a magnetic field gradient. Magnetophoresis consists of measuring the migration speed of magnetic cells suspended in a medium of known viscosity (23). After incubation and recovery, cells were centrifuged at 1200 rpm for 10 min, then diluted in RPMI (10⁴ cells/mL), and 400 μ L of sample was placed in a Hellma chamber 1 mm thick. Cell displacement in steady-state conditions was videotaped with a camera assembled on the microscope, and the movies were treated with dedicated image software (NIH, Bethesda, MD). The diameter and displacement of 30–50 cells were analyzed per assay, yielding the mean cell diameter and cell velocity distribution. The number of particles per cell was calculated using the equation described in Ref. 23 with: the number $N = (3\pi\eta D) / (m_{eff}(dB/dz)) v$ with the viscosity $\eta = 10^{-3}$ Poiseuille, D the cell diameter, v the cell speed, $m_{eff} = 8 \times 10^{-20}$ A.m the effective magnetic moment of a particle in the field ($B = 174$ mT) and the magnetic field gradient $(dB/dz) = 18.5$ mT/mm. The number of iron atoms per particle being known (13,700 atoms), it was possible to calculate the iron mass per cell, as m (pg) = $N \times 1.28 \times 10^6$.

Electron Spin Resonance

ESR was used as described in Ref. 23 to quantify the number of maghemite nanoparticles in a cell sample.

After incubation with particles, cells were centrifuged for 10 min at 1200 rpm and the cell pellet was resuspended in 50 μ L of citrated RPMI medium. Samples of 2 μ L were diluted in 98 μ L of RPMI and introduced in a Malassez slide for cell counting under a light microscope. A 2- μ L aliquot was sampled with a 10- μ L diameter capillary tube (WiretrollII, Drummond Scientific, Broomall, PA). The tube was maintained vertically for 3 days to permit cell sedimentation, then placed in a quartz tube for ESR measurement. The ESR apparatus was first calibrated with ferrofluid samples of known concentrations. The mean iron mass per cell was estimated from the iron mass and the number of cells in the sample.

Quantification of Iron Load After Cell Division

On day 1, hybridomas were incubated for 20 min with either 5 or 15 mM iron, then iron load was estimated, cells were counted, and viability was measured with the Trypan blue test; the cells were then cultured. The same procedure was repeated on day 3.

Injection of Labeled Cells *In Vivo*

The labeling conditions were [Fe] = 8 mM, 20 min incubation time, and 1 hr of chase. Hybridomas were collected by scraping in citrated RPMI, counted, and tested with Trypan blue. They were centrifuged at 1200 rpm for 10 min and the cell pellet was resuspended by aspiration-repression in a volume of RPMI yielding a cell density from 10×10^4 to $15 \times 10^4/\mu$ L. Twenty million labeled hybridoma cells were injected *i.p.* into 1-month-old male Swiss nude mice (Iffa Credo, l'Arbresle, France). The animals were imaged 24 hr after injection. Six mice injected

with magnetically labeled hybridomas and 7 control (not injected) mice were used.

MRI

MRI was performed on a 1.5 T apparatus (Signa, General Electric Medical Systems, Milwaukee, WI) at the Centre Inter Etablissement de Résonance Magnétique (CIERM, Hôpital Kremlin Bicêtre, Paris, France). A dedicated antenna for small animals was used. Animals were anesthetized with a mixture of xylazine (Rompum 2%, Bayer pharma, Puteaux, France) and ketamine (Imalgene 500, Merial, Lyon, France) diluted in normal saline (Rompum: 5% final volume; Imalgene: 20% final volume) and injected by the i.p. route at a dose of 10 $\mu\text{L/g}$ of mouse weight. Once anesthetized, animals were placed in a tube with an oil phantom. The tube was placed in the antenna and then positioned at the center of the magnet. T_1 (TR = 500 ms, TE = 13 ms, field of view (cm) = 4×4 , acquisition matrix = 256×192 , thickness = 1 mm) and T_2 (TR = 2000 ms, TE = 20 and 60 ms) weighted spin echo and gradient echo (GRE) (TR = 20 ms, TE = 4 ms, flip angle = 30°) sequences were acquired.

Images were analyzed with eFilmLite software (Merge eFilm, Netherlands). Several regions of interest (ROIs) were positioned manually at the level of the spleen, giving the signal intensity (SI). The relative signal intensities (RI) were calculated by dividing the SI values by those of the oil phantom: $RI_{spleen} = SI_{spleen} / SI_{oil}$. The enhancement (ENH) was calculated as: $ENH (\%) = (RI_{spleen} - RI_{control}) / RI_{control} \times 100$.

Ex Vivo Recovery of Labeled Cells

After image acquisition, the animals were killed by anesthetic overdose. The spleen was removed and maintained in RPMI at 4°C , then dissociated in this medium using a Potter homogenizer. The cell suspension was filtered on medical gauze saturated with RPMI medium. The cells were washed with RPMI by two centrifugation steps at 1200 rpm for 10 min, and erythrocytes were eliminated by adding hypertonic buffer (NH_4Cl 0.155 M; KHCO_3 0.01 M; EDTA 10^{-4} M) for 5 min. The reaction was stopped by adding a large volume of complete medium and the cells were washed again as described above. A mouse spleen yields from 60 to 100 million splenocytes (leukocytes). The collected cell population was analyzed by magnetophoresis and ESR. Magnetophoresis gave the quantity of iron in labeled cells and ESR the total quantity of iron in the sample. Knowing the number of cells contained in the sample measured by ESR, we calculated the proportion of labeled cells present in the spleen.

RESULTS

Cellular Uptake: Concentration and Time Dependence

In each experimental condition, magnetophoresis showed a homogeneous velocity distribution, consistent with homogeneous labeling of the cell population.

Quantitative studies showed, for each incubation time (20 min and 2 hr), that the number of particles in cells was dependent on the iron concentration in the incubation

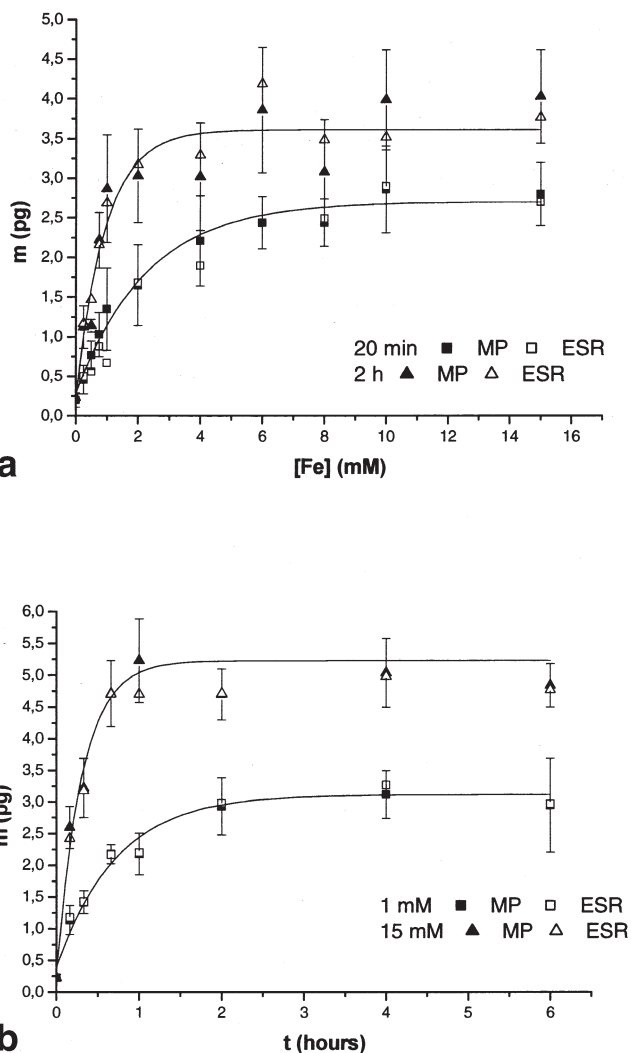


FIG. 1. Magnetophoresis (MP) and ESR quantification of magnetic nanoparticle uptake by hybridoma cells. **a**: Iron mass internalized per cell after 20 min and 2 hr of incubation, as a function of the extracellular iron concentration [Fe]. **b**: Time course of nanoparticle internalization (iron mass per cell) for [Fe] = 1 mM and 15 mM. Exponential guides are shown as solid lines.

medium. Cells showed saturable uptake: up to 2.8 ± 0.4 pg per cell at 20 min and up to 4 ± 0.6 pg per cell at 2 hr (Fig. 1a). Cell labeling was carried out in the same conditions on a population of splenic cells (data not shown). As with hybridomas, the number of particles internalized by splenocytes increased with the iron concentration in the incubation medium, and then reached a plateau. By comparison with hybridomas, maximum masses of iron incorporated in splenocytes were lower (1.1 ± 0.2 pg vs. 2.8 ± 0.4 pg per cell at 20 min, 1.4 ± 0.1 pg vs. 4 ± 0.6 pg per cell at 2 hr).

For a given iron concentration in the incubation medium (1 mM or 15 mM), the iron mass incorporated by hybridoma cells increased with time, towards an equilibrium value of 3.1 ± 0.4 pg per cell at [Fe] = 1 mM, and 5 ± 0.5 pg per cell at [Fe] = 15 mM (Fig. 1b).

In all these studies, viability exceeded 98% in the Trypan blue exclusion test. Only in extreme labeling con-

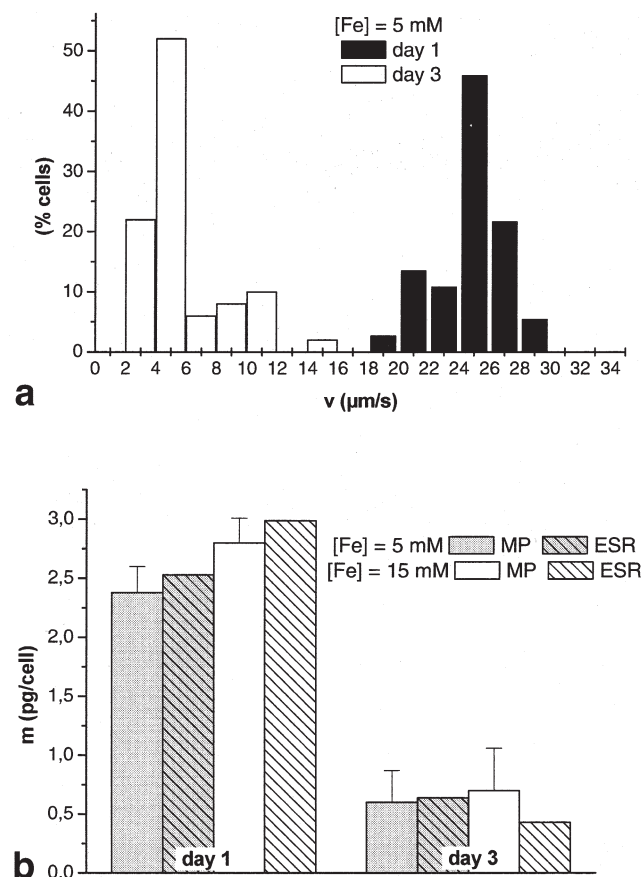


FIG. 2. Effect of cell division on magnetic load. **a**: Cell velocity measurements by magnetophoresis. Two conditions of magnetic labeling were carried out with hybridomas cells, $[\text{Fe}] = 5 \text{ mM}$ and 15 mM (not shown in **a**) in the incubation medium, for 20 min. There was a shift towards lower velocities on day 3, indicating homogeneous distribution of the magnetic load in daughter cells. **b**: Iron quantification on day 1 and day 3 by magnetophoresis (MP) and electron spin resonance (ESR) in the two labeling conditions.

ditions (4 hr and 6 hr with 15 mM iron) was cell viability lower (96% and 93%, respectively).

In both time- and concentration-effect experiments, iron mass measured by magnetophoresis and ESR gave very similar quantitative results (Fig. 1a,b).

Iron Load After Cell Division

In this study the labeling conditions were $[\text{Fe}] = 5 \text{ mM}$ and 15 mM , for 20 min and 1 hr of chase. The iron load per cell was measured by magnetophoresis and ESR on the day of labeling (day 1) and after 48 hr (day 3). In the two labeling conditions, cells showed a Gaussian velocity distribution on day 1, with a mean velocity of $24.6 \pm 2.3 \mu\text{m/s}$ at 5 mM and $28.8 \pm 2.2 \mu\text{m/s}$ at 15 mM (Fig. 2a). On day 3 the velocity distribution shifted towards lower values, with mean velocities of $5.9 \pm 2.8 \mu\text{m/s}$ and $6.9 \pm 3.7 \mu\text{m/s}$ at 5 mM and 15 mM , respectively (Fig. 2a). A slight broadening of the velocity distribution was observed in each case. The iron mass per cell fell between day 1 and day 3 by a factor of 4 ($2.4 \pm 0.2 \text{ pg}$ vs. $0.6 \pm 0.3 \text{ pg}$ per cell at 5 mM , $2.8 \pm 0.2 \text{ pg}$ vs. $0.7 \pm 0.4 \text{ pg}$ per cell at 15 mM) (Fig.

2b). The cell population always increased by a factor of 16 between the first and third day of study, corresponding to about four divisions (2^4), a value in keeping with the known division time of hybridomas. The proliferation of labeled cells in both conditions was the same as that of unlabeled control cells. Cell mortality (Trypan blue test) never exceeded 2–3%. In addition, magnetophoresis and ESR measurements of the iron mass per cell correlated well (Fig. 2b).

In Vivo Studies

Twenty-four hours after injection of magnetically labeled hybridomas (2.5 pg iron per cell), a dark spleen signal was observed on 1.5 T MRI images relative to noninjected control mice (Fig. 3). The quantitative study showed a significant decrease in signal intensity on all sequences. On average, the signal decrease ranged from $-29.2 \pm 13.6\%$ on T_1 , $-24.3 \pm 13.4\%$ on GRE, and $-31.6 \pm 15.9\%$ and $-47.3 \pm 23.8\%$ (first and second echoes) on T_2 -weighted sequences. This suggested a “homing” of magnetically labeled hybridomas to the spleen.

Ex Vivo Studies

After imaging studies, spleens were harvested and splenic cells were studied by magnetophoresis. Two populations were identified. The first population, with a diameter corresponding to splenocytes ($7\text{--}8 \mu\text{m}$), was static and adhered quickly to the bottom of the Hellma chamber. The second population migrated in the magnetic field gradient and had a diameter corresponding to that of hybridomas, albeit slightly smaller than in vitro ($10 \mu\text{m}$, vs. $12 \mu\text{m}$ in vitro). The migration speed of these cells appeared homogeneous from one spleen to another. Iron mass per cell averaged $0.78\text{--}0.96 \text{ pg}$, depending on the sample (Table 1). This value corresponded to the iron mass for a hybridoma after labeling (2.5 pg iron per cell), and after 1 to 2 cellular divisions.

Total iron mass was deduced from ESR values (Table 1). The number of cells in the sample and the iron mass per cell being known (from the magnetophoresis assay), it was possible to calculate the percentage of magnetically labeled cells in the spleen. This value ranged from 2.3% for mouse 3–17.4% for mouse 4. The total number of cells in the spleen being known, it was possible to calculate the number of hybridomas present within the spleen at the time of excision (Table 1). The spleen negative enhancement correlated with the proportion of labeled cells in the spleen (Table 2).

DISCUSSION

This study shows that anionic superparamagnetic nanoparticles are efficiently internalized by hybridoma cells, allowing them to be tracked in the spleen by 1.5 T MRI after i.p. injection.

Nanoparticle internalization was saturable and dependent on the incubation time and the extracellular particle concentration. After 2 hr incubation with 15 mM $[\text{Fe}]$, iron load was $4 \pm 0.6 \text{ pg}$ for hybridomas and $1.4 \pm 0.1 \text{ pg}$ for splenocytes. The kinetics were consistent with a mecha-

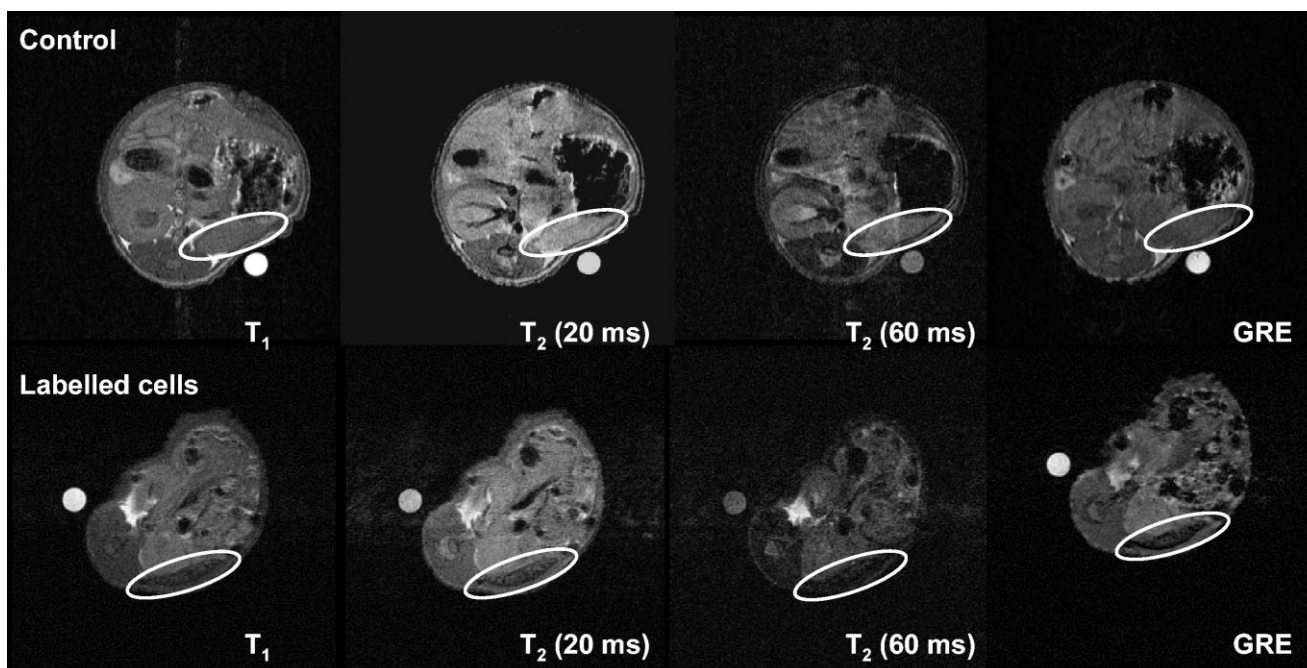


FIG. 3. In vivo 1.5 T MRI. MRI of the spleen of a Swiss nude mouse 24 hr after i.p. injection of magnetically labeled hybridomas (20×10^6) (bottom row), in comparison with uninjected control mice (top row). Sequence weightings (T_1 ; GRE; T_2 first and second echo, respectively) are indicated on the image. The spleen is indicated by an ellipse. A dark spleen signal was obtained relative to the control.

nism involving iron binding to the cell surface. As binding capacity is limited by the cell surface area, iron endocytosis should itself be a function of this area (21). This could explain why hybridomas showed a substantially higher maximal iron load than splenocytes, which are smaller. More generally, different cell types should display different iron load capacities as a function of their surface area. Iron uptake obtained with our anionic particles was much higher than previously reported with dextran-coated particles (i.e., Sinerem) in various tumor cell lines and mouse macrophages, i.e., 0.01–0.12 pg per cell and 0.97 pg per cell, respectively, after 1 hr incubation at 37°C in a suspension containing 2 mM Fe^{3+} (24–26). Thus, within the same short range of labeling periods, we obtained substantial iron mass per cell. The higher internalization capacity of uncoated nanoparticles compared to electrically neutral dextran-coated nanoparticles could be explained by the anionic charge of the former. Electrostatic interactions between charged entities and plasma membranes have been studied for macromolecules such as ferritins (27,28) and liposomes (29–31). Positively charged liposomes were

found to more efficiently bound than their negatively charged counterparts. This is consistent with the results of electrophoresis studies showing that the plasma membrane has a total negative charge. However, it has been shown that small anionic tracer peptides can nevertheless label the cellular membrane and be internalized by the endocytosis pathway, proving the existence of cation sites on the cell surface (32). Cation site-bound anionic nanoparticles are thought to form clusters due to electrostatic repulsion by the negative charges of the plasma membrane, before being internalized by the endocytosis pathway. Indeed, endosomes containing nanoparticles are observable by electron microscopy (23).

Although based on different physical principles, magnetophoresis and ESR gave similar nanoparticle uptake values. Magnetophoresis measures the velocity of magnetically labeled cells in suspension. Its main limitation concerns cells with a low iron load. These cells descend in the Hellma chamber, forming a deposit of nonmigrating cells. Another limitation is that measurement requires high dilution of the sample. Indeed, the hydrodynamic flow

Table 1
Iron mass per hybridoma cell in the spleen (ex vivo studies)

Mouse number	1	2	3	4	5	6
Iron mass per cell (pg) (magnetophoresis)	0.96	0.89	0.86	0.78	0.87	0.87
Total iron mass (pg) in ESR sample	79,750	95,700	14,200	66,400	69,800	69,800
Labeled hybridomas (%) in the spleen	13.8	13.3	2.3	17.4	13.6	9.5
Number of labeled ($\times 10^6$) hybridomas in the spleen	8.4	9.1	1.3	13.6	14.5	6.0

Iron mass, as measured by magnetophoresis (MP), was consistent with hybridoma division after incubation for 20 min in the presence of $[\text{Fe}] = 8 \text{ mM}$. The proportions of labeled hybridomas in the spleen were deduced from ESR and MP values, knowing the total number of cells in the spleen and in the sample. The number of labeled hybridomas in the spleen was calculated from the total splenocyte population.

Table 2
Spleen negative enhancement on the different MRI sequences and the percentage of labeled splenic cells ex vivo

% cells	Mouse 3 (2.3%)	Mouse 6 (9.5%)	Mouse 2 (13.3%)	Mouse 5 (13.6%)	Mouse 1 (13.8%)	Mouse 4 (17.4%)
T_1	-6.6 ± 0.7	-26.2 ± 3.2	-39.6 ± 3.8	-37.9 ± 18.8	-42.5 ± 3	-22.5 ± 1
GRE	-8.6 ± 3.7	-14.4 ± 6.9	-41.8 ± 12.7	-16.1 ± 14.9	-36.9 ± 18.7	-28.1 ± 11.1
T_2 (20 ms)	-10.7 ± 6.3	-13.2 ± 0.1	-47.9 ± 2.4	-33.4 ± 5.1	-43.6 ± 0.8	-41 ± 1.4
T_2 (60 ms)	-14.2 ± 0.4	-20.7 ± 6.9	-69.4 ± 9.7	-55.4 ± 0.1	-57.1 ± 3.9	-66.7 ± 4.4

The proportion of labeled hybridomas in the sample was deduced from ESR and MP measurements of cells in the spleen. Spleen negative enhancement (in %) on the different sequences correlated with the proportion of labeled cells recovered from the spleen.

formed by cells in migration can disturb the migration of neighboring cells. In practice, we were able to assay samples containing as few as 30–50 cells/ μL and about 0.2 pg of iron per cell, moving at a minimum speed of 2 $\mu\text{m/s}$. ESR can be used to quantify the electron spins contained in a small sample of low volume with a detection threshold of 2×10^9 ferromagnetic particles or 2×10^3 pg of iron particles per sample. We found a good correlation between the two methods as regards cellular quantification. This provides indirect evidence that the migration speed of nanoparticles under the magnetic field is related to the number of internalized particles. Thus, magnetophoresis could be a simple and precise method to quantify the uptake of any kind of magnetic particle internalized by a variety of cells. Similarly, ESR can be used to quantify iron not only in cells but also in tissue samples to study marker biodistribution.

We used these two methods to study particle distribution during the course of cell division. With magnetophoresis, cell velocity histograms suggested that internalized nanoparticles were equally distributed among daughter cells during division. The cell population increased by a factor of 16 in both labeling conditions, corresponding to four cell divisions (2^4). In theory, if labeling endosomes are divided equally between daughter cells, iron mass per cell should be reduced by a factor 16, i.e., 0.15 pg and 0.17 pg per cell at day 3 in 5 mM and 15 mM Fe labeling conditions, respectively. However, we only found a 4-fold reduction. Several factors might explain this result. First, the quantification methods used here are more efficient for strongly labeled cells and are not sensitive to low values. An iron load of 0.15 pg is close to the detection threshold of 0.2 pg. Second, strongly labeled cells may divide more slowly than weakly labeled cells. No cell toxicity was observed in the Trypan blue exclusion test up to 3 days after labeling. Beyond this time, iron mass became undetectable by magnetophoresis. In addition, no difference in antibody secretion between labeled and control hybridomas was observed by FACS analysis (data not shown). This result supports that cell function is not affected by cell labeling. Owing to the rapid division of hybridomas, further viability studies were not performed, iron no longer being detectable. The potential long-term toxicity of iron labeling should be studied at later times using more slowly dividing cell types.

Once magnetically labeled, hybridomas were detectable in vivo by MRI after i.p. injection. Injection of labeled hybridomas resulted in a darkening of the spleen on all sequences, both T_2 - and T_1 -weighted. This darkening was more pronounced on T_2 -weighted images. The negative

enhancement obtained after homing of labeled hybridomas to the spleen was attributed to the effect of magnetic nanoparticles on T_2 and T_2^* contrasts. Indeed, anionic nanoparticles are compartmentalized in endosomes and lysosomes and behave as aggregated particles. Aggregated particles exhibit a decrease in r_1 , and a slight decrease in r_2 relaxivities compared to free particles, resulting in negative contrast on T_1 - and T_2 -weighted images (33). We used GRE-weighted images to optimize the darkening of the spleen.

Magnetically labeled cells were recovered from the spleen in order to confirm that the negative MRI enhancement was effectively due to labeled hybridomas and not to free nanoparticles present in the spleen. Moreover, these labeled cells retained their proliferative capacity in vivo, as the iron content of hybridomas recovered from the spleen was much lower than that of the hybridomas initially injected. As shown in Table 2, we found a correlation between MRI results and the percentage of labeled cells found in the spleen after ex vivo measurement by ESR and magnetophoresis. The spleen of the mouse showing weak negative MRI enhancement contained an estimated 2.3% of labeled cells. In contrast, the spleen of the mouse with strong negative enhancement contained 17.4% of labeled cells. The hyposignal resulting from interaction of the anionic nanoparticles with the local magnetic field in the spleen was not optimized, but corresponded to about 2.3% (1.3 million cells) in the spleen, as determined using a clinical imaging system. Thus, quantitative MR imaging data can be obtained with the techniques capable of quantifying the number of labeled cells in a target organ.

CONCLUSION

From the present results on hybridomas, we suggest that anionic nanoparticles ($\gamma\text{-Fe}_2\text{O}_3$) could serve as an efficient and useful marker for in vivo quantitative imaging of injected tracer cells on a 1.5 T MRI device. The suitability of our labeling technique to approach lymphocyte and stem cell tracking in vivo will be the matter of future studies.

ACKNOWLEDGMENTS

We thank Pr. Jacques Bittoun (CIERM, Centre Inter Etablissement de Résonance Magnétique, Hôpital Kremlin Bicêtre, Paris, France) for helpful discussions, and Dr. Sophie Ezine and Dr. Claire Wilhelm for scientific discussions and technical support. We thank Dr. Flora Zavala for

scientific advice, and Dr. Christine Menager for providing the particles.

REFERENCES

- Wallace PK, Palmer LD, Perry-Lalley D, Bolton ES, Alexander RB, Horan PK, Yang JC, Muirhead KA. Mechanisms of adoptive immunotherapy: improved methods for in vivo tracking of tumor-infiltrating lymphocytes and lymphokine-activated killer cells. *Cancer Res* 1993;53(10 Suppl):2358–2367.
- Hanto DW, Hopt UT, Hoffman R, Simmons RL. Recruitment of unsensitized circulating lymphocytes to sites of allogeneic cellular interactions. *Transplantation* 1982;33:541–546.
- Potsch C, Vohringer D, Pircher H. Distinct migration patterns of naive and effector CD8 T cells in the spleen: correlation with CCR7 receptor expression and chemokine reactivity. *Eur J Immunol* 1999;29:3562–3570.
- De Becker G, Moulin V, Pajak B, Bruck C, Francotte M, Thiriart C, Urbain J, Moser M. The adjuvant monophosphoryl lipid A increases the function of antigen-presenting cells. *Int Immunol* 2000;12:807–815.
- Fisher B, Packard BS, Read EJ, Carrasquillo JA, Carter CS, Topalian SL, Yang JC, Yolles P, Larson SM, Rosenberg SA. Tumor localization of adoptively transferred indium-111 labeled tumor infiltrating lymphocytes in patients with metastatic melanoma. *J Clin Oncol* 1989;7:250–261.
- Bulte JW, Laughlin PG, Jordan EK, Tran VA, Vymazal J, Frank JA. Tagging of T cells with superparamagnetic iron oxide: uptake kinetics and relaxometry. *Acad Radiol* 1996;3(Suppl 2):S301–303.
- Weissleder R, Moore A, Mahmood U, Borhade R, Benveniste H, Chiozza EA, Basilion JP. In vivo magnetic resonance imaging of transgene expression. *Nat Med* 2000;6:351–355.
- Dodd SJ, Williams M, Suhan JP, Williams DS, Koretsky AP, Ho C. Detection of single mammalian cells by high-resolution magnetic resonance imaging. *Biophys J* 1999;76(1 Pt 1):103–109.
- Yeh TC, Zhang W, Ildstad ST, Ho C. In vivo dynamic MRI tracking of rat T-cells labeled with superparamagnetic iron-oxide particles. *Magn Reson Med* 1995;33:200–208.
- Jung CW. Surface properties of superparamagnetic iron oxide MR contrast agents: ferumoxides, ferumoxtran, ferumoxsil. *Magn Reson Imag* 1995;13:675–691.
- Vives E, Brodin P, Lebleu B. A truncated HIV-1 Tat protein basic domain rapidly translocates through the plasma membrane and accumulates in the cell nucleus. *J Biol Chem* 1997;272:16010–16017.
- Rusnati M, Tarabozetti G, Urbinati C, Tulipano G, Giuliani R, Molinari-Tosatti MP, Sennino B, Giacca M, Tyagi M, Albini A, Noonan D, Giavazzi R, Presta M. Thrombospondin-1/HIV-1 tat protein interaction: modulation of the biological activity of extracellular Tat. *FASEB J* 2000;14:1917–1930.
- Josephson L, Tung CH, Moore A, Weissleder R. High-efficiency intracellular magnetic labeling with novel superparamagnetic-Tat peptide conjugates. *Bioconjug Chem* 1999;10:186–191.
- Lewin M, Carlesso N, Tung CH, Tang XW, Cory D, Scadden DT, Weissleder R. Tat peptide-derivatized magnetic nanoparticles allow in vivo tracking and recovery of progenitor cells. *Nat Biotechnol* 2000;18:410–414.
- Bulte JW, Zhang S, van Gelderen P, Herynek V, Jordan EK, Duncan ID, Frank JA. Neurotransplantation of magnetically labeled oligodendrocyte progenitors: magnetic resonance tracking of cell migration and myelination. *Proc Natl Acad Sci USA* 1999;96:15256–15261.
- Bulte JW, Douglas T, Witwer B, Zhang SC, Strable E, Lewis BK, Zywicke H, Miller B, van Gelderen P, Moskowitz BM, Duncan ID, Frank JA. Magnetodendrimers allow endosomal magnetic labeling and in vivo tracking of stem cells. *Nat Biotechnol* 2001;19:1141–1147.
- Hoehn M, Kustermann E, Blunk J, Wiedermann D, Trapp T, Wecker S, Focking M, Arnold H, Hescheler J, Fleischmann BK, Schwindt W, Buhle C. Monitoring of implanted stem cell migration in vivo: a highly resolved in vivo magnetic resonance imaging investigation of experimental stroke in rat. *Proc Natl Acad Sci USA* 2002;99:16267–16272.
- Halbreich A, Roger J, Pons JN, Geldwerth D, Da Silva MF, Roudier M, Bacri JC. Biomedical applications of maghemite ferrofluid. *Biochimie* 1998;80:379–390.
- Fauconnier N, Pons JN, Roger J, Bee A. Thiolation of maghemite nanoparticles by dimercaptosuccinic acid. *J Colloid Interface Sci* 1997;194:427–433.
- Bacri JC, Perzynski R, Salin D, Cabuil V, Massart R. Magnetic colloidal properties of ionic ferrofluids. *J Mag Mag Mat* 1986;62:36–46.
- Wilhelm C, Billotey C, Roger J, Pons JN, Bacri JC, Gazeau F. Intracellular uptake of anionic superparamagnetic nanoparticles as a function of their surface coating. *Biomaterials* 2003;24:1001–1011.
- Massart R. *IEEE Trans Magn* 1981;17:1247.
- Wilhelm C, Gazeau F, Bacri JC. Magnetophoresis and ferromagnetic resonance of magnetically labeled cells. *Eur Biophys J* 2002;31:118–125.
- Schulze E, Ferrucci JT Jr, Poss K, Lapointe L, Bogdanova A, Weissleder R. Cellular uptake and trafficking of a prototypical magnetic iron oxide label in vitro. *Invest Radiol* 1995;30:604–610.
- Moore A, Weissleder R, Bogdanov A Jr. Uptake of dextran-coated monocrySTALLINE iron oxides in tumor cells and macrophages. *J Magn Reson Imag* 1997;7:1140–1145.
- Moore A, Marecos E, Bogdanov A Jr, Weissleder R. Tumoral distribution of long-circulating dextran-coated iron oxide nanoparticles in a rodent model. *Radiology* 2000;214:568–574.
- Farquhar MG. Recovery of surface membrane in anterior pituitary cells. Variations in traffic detected with anionic and cationic ferritin. *J Cell Biol* 1978;77:R35–42.
- Mutsaers SE, Papadimitriou JM. Surface charge of macrophages and their interaction with charged particles. *J Leukoc Biol* 1988;44:17–26.
- Lee KD, Nir S, Papahadjopoulos D. Quantitative analysis of liposome-cell interactions in vitro: rate constants of binding and endocytosis with suspension and adherent J774 cells and human monocytes. *Biochemistry* 1993;32:889–899.
- Miller CR, Bondurant B, McLean SD, McGovern KA, O'Brien DF. Liposome-cell interactions in vitro: effect of liposome surface charge on the binding and endocytosis of conventional and sterically stabilized liposomes. *Biochemistry* 1998;37:12875–12883.
- Chenevier P, Veyret B, Roux D, Henry-Toulme N. Interaction of cationic colloids at the surface of J774 cells: a kinetic analysis. *Biophys J* 2000;79:1298–1309.
- Ghinea N, Simionescu N. Anionized and cationized hemeundecapeptides as probes for cell surface charge and permeability studies: differentiated labeling of endothelial plasmalemmal vesicles. *J Cell Biol* 1985;100:606–612.
- Billotey C, Wilhelm C, Devaud M, Bacri JC, Bittoun J, Gazeau F. Cell internalization of anionic maghemite nanoparticles: Quantitative effect on magnetic resonance imaging. *Magn Reson Med* 2003;49:646–654.